

Dithiocarbamate Anchoring in Molecular Wire Junctions: A First Principles Study

Zhenyu Li and Daniel S. Kosov

*Department of Chemistry and Biochemistry,
University of Maryland, College Park, 20742*

Abstract

Recent experimental realization [J. Am. Chem. Soc., 127 (2005) 7328] of various dithiocarbamate self assembly on gold surface opens the possibility for use of dithiocarbamate linkers to anchor molecular wires to gold electrodes. In this paper, we explore this hypothesis computationally. We computed the electron transport properties of 4,4'-bipyridine (BP), 4,4'-bipyridinium-1,1'-bis(carbodithioate) (BPBC), 4-(4'-pyridyl)-peridium-1-carbodithioate (BPC) molecule junctions based on the density functional theory and non-equilibrium Green's functions. We demonstrated that the stronger molecule-electrode coupling associated with the conjugated dithiocarbamate linker broadens transmission resonances near the Fermi energy. The broadening effect along with the extension of the π conjugation from the molecule to the gold electrodes lead to enhanced electrical conductance for BPBC molecule. The conductance enhancement factor is as large as 25 at applied voltage bias 1.0 V. Rectification behavior is predicted for BPC molecular wire junction, which has the asymmetric anchoring groups.

arXiv:cond-mat/0702623v1 [cond-mat.mtrl-sci] 27 Feb 2007

I. INTRODUCTION

Considerable experimental and computational efforts have been devoted in recent years to the problem of molecular electronics.^{1,2} These efforts have been spurred on by the anticipation for breakthrough technological applications. When an electronic devices shrink to molecular level, the molecule-electrode contact becomes a major part of the device and chemical details of the bonding becomes pivotal for the device electron transport properties.^{3,4,5,6} To date, the most widely used molecular wire junctions have been formed by thiolated molecules assembled between gold electrodes. There is growing experimental awareness of the fact that one of the most important challenges in molecular-scale electronics is the ill-defined bonding between molecular wires and gold electrodes. The aim of the reproducible experimental measurements has become the search for better molecule-electrode bonding.^{7,8,9,10,11,12} Most of recent experiments has attempted to circumvent shortcomings of thiol linkage by using carbenes on transition metals⁷ and on metal carbides⁸, by inserting molecular wires into nanogaps in single-walled carbon nanotubes¹⁰, or by fabricating metal-free silicon-molecule-nanotube molecular devices.¹² But being an excellent conductor with mature manipulation technics, gold remains one of the most attractive electrode material for molecular electronics.

It has been recently shown by Zhao *et al.*¹³ that dithiocarbamate formation provides a reliable technology for conjugating secondary amines onto metal surfaces to form strongly absorbed molecular ligands which are stable under various types of the environmental stress. This result suggests a possibility of connection of molecular wires to gold electrodes via dithiocarbamate group instead of thiol group. In fact, the distance between the sulphur atoms in the dithiocarbamate group is nearly ideal for epitaxial adsorption onto Au surface, and a variety of secondary amines can condense with dithiocarbamate linker onto Au surfaces at room temperature,¹³ which makes the dithiocarbamate anchoring structure to be easily fabricated and characterized. On the other hand, the dithiocarbamate anchoring group provides strong molecule-electrode coupling, and thus the possibility of more stable junctions with enhanced conductance.

Theoretically, stronger molecule-electrode coupling leads to more significant manifestation of the effects associated with the molecule-electrode interface. The substantial charge transfer may occur between the molecule and the metal electrodes even in the absence of

the applied field upon initial chemisorption and it will determine the transport properties of the molecular wire junctions. The stronger is the molecule-electrode coupling, the larger is the mixing between the discrete molecular levels and the continuum of the metal electronic states and the larger is the broadening of the resonances in the electron transmission probability. The dithiocarbamate anchoring group thus provides an ideal testing ground for computational and experimental explorations of the role of such pivotal effects in the transport properties of molecular wires.

Dithiocarbamate assembly on the gold surface also opens interesting possibility for creating rectifying molecular wire junctions where electrons flow along one preferential direction.¹⁴ A number of donor-acceptor type molecular rectifiers has been proposed,^{14,15,16,17,18} in which the electron density asymmetry (like in semiconductor p-n junctions) causes the current to flow in one direction. Rectification effect could also be achieved by adjusting the molecule-electrode bond length as it was suggested theoretically,¹⁹ but it is difficult to realize such kind of the rectifying molecular wire junctions in a controllable way. We propose that molecular rectification can be realized in a more practical way by choosing different anchoring group for the left and the right sides.

The aim of this paper is to explore computationally the role of dithiocarbamate anchoring group on transport properties of molecular wire junctions. In this paper, we consider three systems as prototype molecular wire junctions: two symmetric molecular wires 4,4'-bipyridine (BP) and 4,4'-bipyridinium-1,1'-bis(carbodithioate) (BPBC), and one asymmetric junction 4-(4'-pyridyl)-peridium-1-carbodithioate (BPC). We choose the bipyridine based molecular wire junctions because its transport properties have been thoroughly characterized, both experimentally^{20,21} and theoretically^{22,23,24}. With two nitrogen atoms at the two opposite ends, BP is able to connect to gold electrode directly. By repeatedly forming thousands of molecular junctions between gold scanning tunneling microscope tip and a gold substrate in solution, Xu *et al.*²¹ found the conductance of BP molecule near zero bias was about 0.01 G_0 , where $G_0 = e^2/\pi\hbar = 77.48\mu S$ is the quantum of conductance. Theoretically, the conductance of directly linked BP molecular wire has been calculated non-self-consistently by both cluster²² and bulk electrode model.²³ Very recently, a more precise fully self-consistent non-equilibrium Green's functions (NEGF) calculation has also been performed on this system.²⁴ In this paper, we perform combined density functional theory (DFT) and NEGF calculations on the electron transport properties of BP,BPBC,

and BPC. The electric current at finite bias voltage is determined self-consistently in our calculations. We find that dithiocarbamate linkers yield significant broadening of peaks in the transmission spectra and improve significantly electron transport properties of molecular wire junctions. We suggest and confirm computationally that BPC molecular wire junction rectifies (with factor close to 2) the electric current which flows through.

II. COMPUTATIONAL METHODS

The electronic transport properties are calculated with the NEGF technique using TranSIESTA-C package (version 1.3.0.4).²⁵ In this package, the molecular wire junction is divided into three regions, left electrode (L), contact region (C), and right electrode (R). The contact region typically includes parts of the physical electrodes where the screening effects take place, to ensure that the charge distributions in L and R region correspond to the bulk phases of the same material. The semi-infinite electrodes (Au(111)-(3×3) surfaces in our case) are calculated separately to obtain the bulk self-energy.

The main loop for self-consistent NEGF/DFT calculations is described below. For detailed description and for the technical details suppressed here we refer to the paper of Brandbyde *et al.*²⁵ The Green's function is computed by inverting the finite matrix

$$\mathbf{G}(E, V) = \left[\mathbf{E}\mathbf{S} - \begin{pmatrix} H_L + \Sigma_L & V_L & 0 \\ V_L & H_M & V_R \\ 0 & V_R & H_R + \Sigma_R \end{pmatrix} \right]^{-1}, \quad (1)$$

with V being the applied voltage bias. The matrix product of the Green's function and the imaginary part of the left/right electrodes self-energy yields the spectral densities $\rho^{L/R}(E)$. The spectral densities of the left and right electrodes are combined together to compute the non-equilibrium, voltage-dependent density matrix

$$\mathbf{D} = \int dE [\rho^L(E)f(E - \mu_L) + \rho^R(E)f(E - \mu_R)], \quad (2)$$

where f is Fermi-Dirac occupation numbers. The density matrix is converted into non-equilibrium electron density

$$n(\mathbf{r}) = \sum_{\mu\nu} \phi_{\mu}(\mathbf{r})D_{\mu\nu}\phi_{\nu}(\mathbf{r}), \quad (3)$$

where $\phi_\nu(\mathbf{r})$ atomically localized basis functions. The nonequilibrium electron density enables us to compute matrix elements of the Green's function. The Hartree potential is determined through the solution of the Poisson equation with appropriate voltage dependent boundary conditions. Then this loop of calculations is repeated until self-consistency is achieved. Once the self-consistent convergence is achieved, the transmission spectrum, which gives the probability for electron with incident energy E to be transferred from the left electrode to the right, is calculated by

$$T(E, V) = \text{Tr}[\mathbf{\Gamma}_L(E, V)\mathbf{G}(E, V)\mathbf{\Gamma}_R(E, V)\mathbf{G}^\dagger(E, V)], \quad (4)$$

where $\mathbf{\Gamma}_{L/R}$ is the coupling matrix. The integration of the transmission spectrum yields the electric current:

$$I(V) = \int_{\mu_L}^{\mu_R} T(E, V) (f(E - \mu_L) - f(E - \mu_R)) dE, \quad (5)$$

where $\mu_L = -V/2$ ($\mu_R = V/2$) is the chemical potential of the left(right) electrode.

If we project the self-consistent hamiltonian onto the Hilbert space spanned by the basis functions of the central molecule, we obtain the molecular projected self-consistent hamiltonian (MPSH). The eigenstates of MPSH can be associated with poles of the Green's function and thus roughly correspond to the positions of the peaks in the transmission spectrum (4).

The electronic structure is described within the implementation of DFT in SIESTA computer program,²⁶ which solves the Kohn-Sham equations with numerical atomic basis sets. Double zeta with polarization (DZP) basis set is chosen for all atoms except Au, for which single zeta with polarization (SZP) is used. Our test calculation indicates that using SZP basis set for Au does not effect the accuracy of our calculations. Core electrons are modeled with Troullier-Martins nonlocal pseudopotentials.²⁷ Perdew-Zunger local density approximation (LDA) is used to describe the exchange-correlation potential.²⁸ By comparing the results from two recent calculations with hybrid functional and LDA respectively,^{23,24} we conclude that LDA is adequate in our case.

III. RESULTS AND DISCUSSION

A. Structural models of molecular wire junctions

Transport systems considered in this paper are formed by BP, BPC or BPBC molecules sandwiched between two Au(111)-(3×3) surfaces. Fig. 1 shows the structural models for these molecular wire junctions. Only one unit cell for the semi-infinite left or right electrode is plotted, which contains three Au layers. In the contact region, two Au layers at both left and right side are included, of which the most left and right layers are constrained to their theoretical bulk geometry to match the structure of the Au(111) surface. We assume that all three junctions have coplanar geometry. This narrows down the problem of difference between BP, BPBC, and BPC transport properties to the role of the dithiocarbamate linkers. The rest of the contact region is fully optimized. We also optimized the length of the junctions by computing the potential energy surface (PES, i.e. the energy of the system as a function of the distance between the left and the right electrodes). Every point on the energy surface is calculated by performing a geometry optimization with constrained electrode-electrode distance. Then the PES curve is fitted to determine the correct electrode-electrode distance. We also performed test calculations for non-coplanar BP and BPBC. Twisting of pyridine rings by 10°, which corresponds to equilibrium geometry for the bipyridine junction,²⁴ has negligible influence on the transmission spectra.

Fig. 1a shows the optimized geometry of the BP molecular wire, which is directly connected to two gold electrodes. When BP molecules are adsorbed on gold surface they adopt either atop, hollow, or bridge adsorption sites. Depending upon experimental realization BP molecule may also be connected to the gold surface via apex Au atom. Wu *et al.*²⁴ have studied effects of different interface geometry on the transport properties of BP molecular wire junction, but focused on the hollow site adsorption. Here we study the interface geometry with apex Au atom, which is more likely realized on the typical experiments where gold-molecule-gold junctions were formed by repeated pulling of STM tip from Au surface.²¹ This geometrical configuration also gives the largest value of the conductance.^{6,24} Therefore our calculations predict the lower limit for the enhancement of the conductance by means of dithiocarbamate anchoring. The structural model for BPBC molecular wire junction is shown on Fig.1(b); here each of the four S is connected to the hollow sites of Au(111)-(3×3)

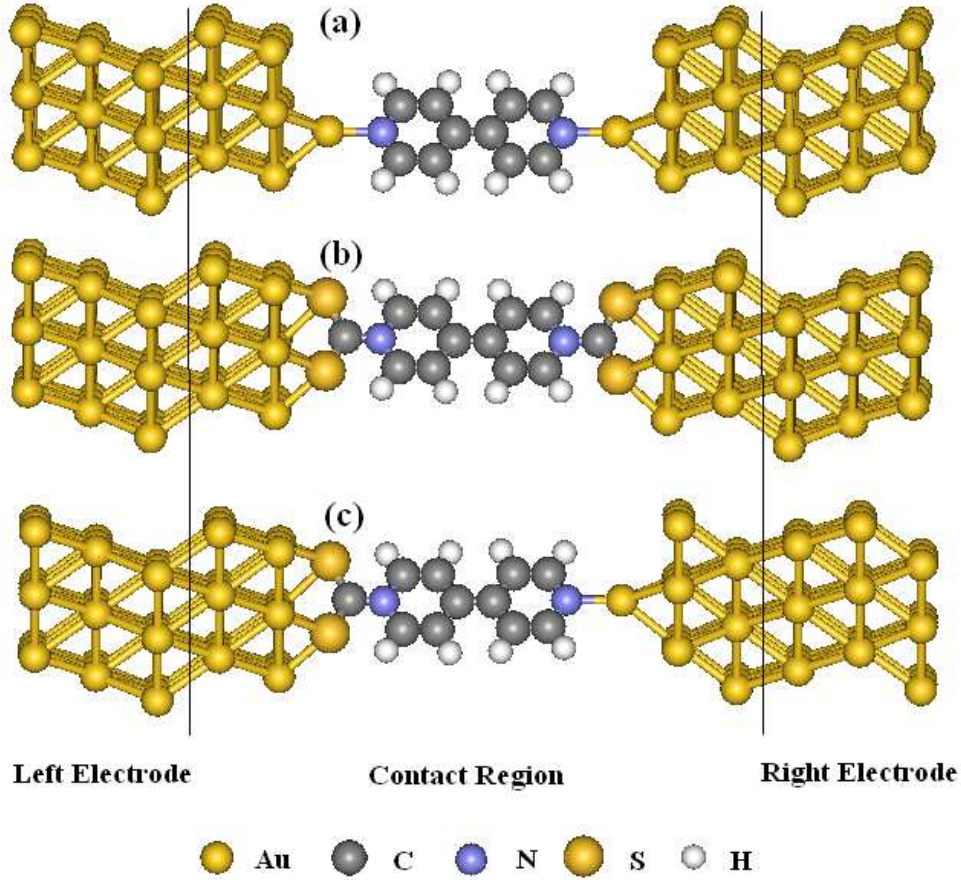


FIG. 1: The relaxed geometry of Au-BP-Au junctions with different anchoring groups. a) BP, b) BPBC, c) BPC.

electrode. This structure resembles the experimental scheme **7** of dithiocarbamate ligands formations on Au surface in Fig. 1 of the paper by Zhao *et al.*¹³ Fig.1(c) shows asymmetric BPC molecule sandwiched between two Au electrodes, in which the left side of the molecule wire is connected via dithiocarbamate linker and the right side is connected via N-Au bond to the apex Au atom.

B. Effect of dithiocarbamate anchoring

To study the effect of dithiocarbamate anchoring, we begin with calculations of the transport properties of BP molecular wire junction. First, we compute the transmission coefficient $T(E)$ (4). The zero bias transmission spectrum of BP junction is shown on Fig.2. The distinctive feature of this transmission is the existence of the narrow resonance which appears

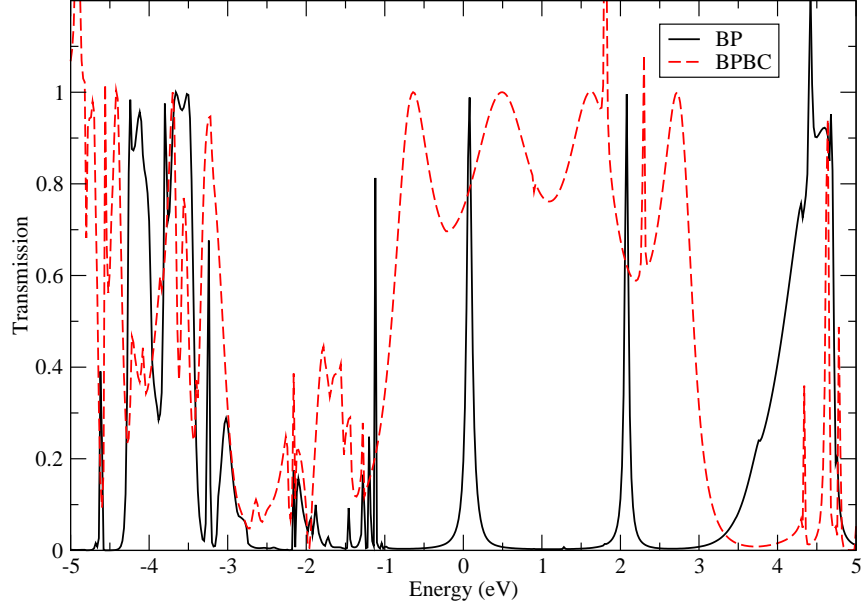


FIG. 2: The transmission spectrum of molecular wire junctions. The average chemical potential of the left and right electrodes is set to zero.

very close to the Fermi level (0.09 eV above E_F). This resonance determines the transport properties of BP molecular wire junction under small bias voltages. Two other narrow peaks are at 2.08 eV above and 1.11 eV below the electrode Fermi energy. The transmission coefficient at the Fermi level (i.e. the conductance at small voltage) is $0.195 G_0$. This computed value of the conductance is by order of magnitude larger than the experimental value of $0.01 G_0$.²¹ But, we notice that the transmission curve from our calculations is consistent with the result of the recent first principles calculations on BP junction,^{6,23,24} if the same interface geometry is considered. In fact, experimental conductance value can be obtained theoretically by choosing a suitable model for the interface geometry.²⁴ Transmission eigenchannel decomposition indicates that the zero voltage conductance is almost entirely determined by a single channel.

The transmission spectrum can be further interpreted in terms of MPSH. The MPSH orbitals near the average Fermi level are plotted on Fig. 3. MPSH orbitals of BP molecular wire junction are very similar to the Kohn-Sham orbitals of an isolated BP molecule except for some additional states which mainly come from apex Au atoms. It indicates that the coupling between BP molecule and apex Au atom is weak, which explains why the resonances in the transmission spectrum are very narrow. Since the resonant peaks in the

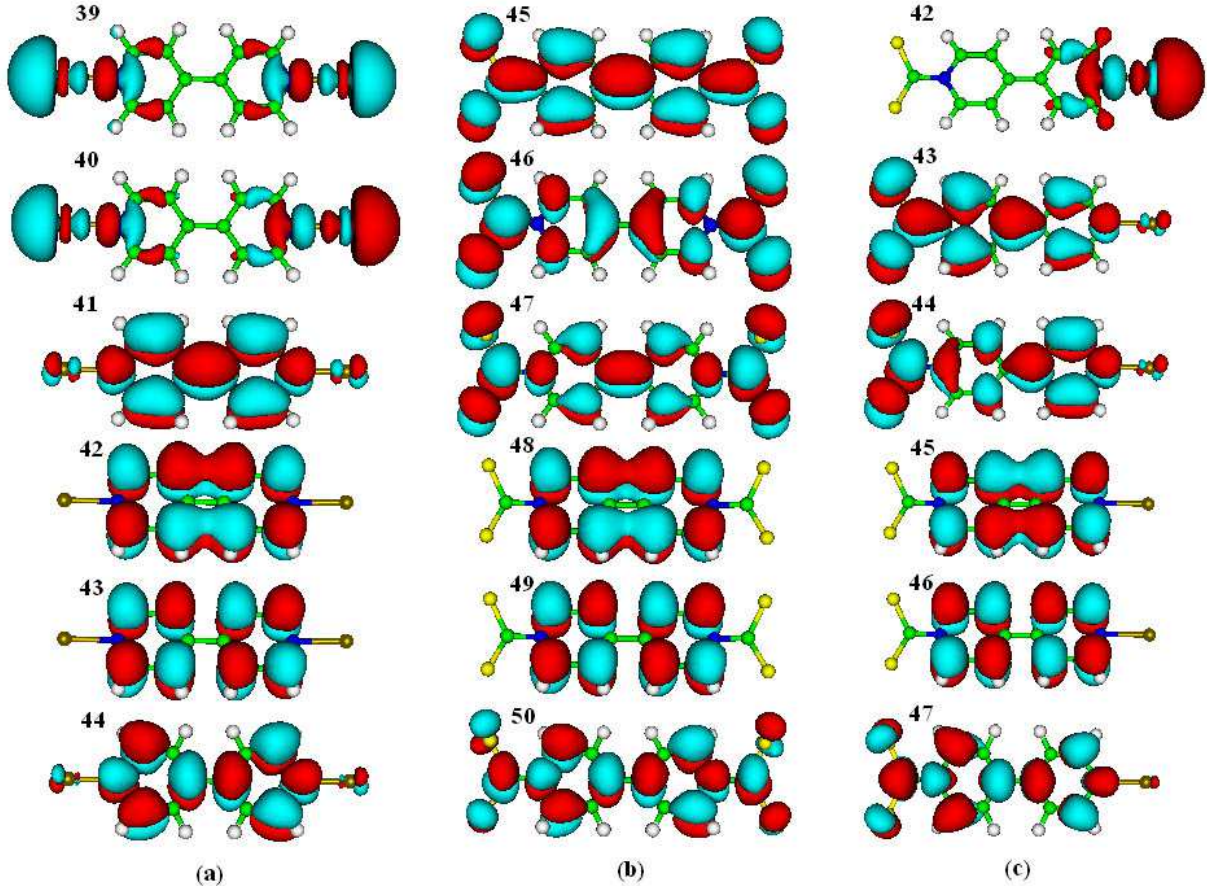


FIG. 3: Eigenstates of MPSH for (a) BP, (b) BPBC, and (c) BPC. Anchoring groups and apex Au atom are included for molecular projection. Refer Fig. 1 for atom types, the atoms are plotted smaller in this figure to present MPSH orbitals better.

transmission are narrow and well separated, it is easy to put them into correspondence with the MPSH orbitals by directly comparing the positions of the resonances with the MPSH eigenenergies. The MPSH eigenenergies are given in Table I. The previously mentioned three peaks correspond to the four MPSH orbitals: they are orbitals 39, 40, 41, and 44. Orbital 39 and 40 are almost degenerated. We can see from Fig. 3a that all these four orbitals have notable density distribution on N atoms.

Since the transport properties of BP molecular wire junction are determined by the narrow resonances in the transmission, experimental measurements could be significantly affected by stochastic switching and could be very sensitive to variations of the electrode-molecule interface. The stochastic switching arises from the structural evolution of the interface geometry. This is undesirable phenomenon, which leads to the changes in the conductance by

TABLE I: Eigenvalues of the molecular projected self-consistent Hamiltonian (MPSH) orbitals. The energy of the average electrode Fermi energy is set to zero.

BP		BPBC		BPC	
n	Energy(eV)	n	Energy(eV)	n	Energy(eV)
35	-2.421	41	-2.759	38	-2.408
36	-2.414	42	-2.746	39	-2.172
37	-2.354	43	-2.542	40	-2.170
38	-2.346	44	-2.510	41	-2.121
39	-1.182	45	-0.851	42	-0.999
40	-1.134	46	0.246	43	-0.340
41	0.044	47	1.474	44	1.234
42	1.285	48	1.786	45	1.890
43	1.806	49	2.276	46	2.377
44	2.050	50	2.643	47	2.677

factors of 2-10 depending upon the scale of the fluctuations.^{5,29,30,31} The "robust" transmission spectrum should possess the following features: a) very broad resonances to reduce the influence of the current-induced fluctuations of the interface geometry; b) large transmission probability in the vicinity of the electrode Fermi energy to make a good conductor from a molecular wire junction.

Dithiocarbamate linker provides strong coupling between the molecular wire and the gold electrode and it continues π -conjugation from the molecule into the gold electrode. Therefore it is very interesting to see if this anchoring group leads to the "robust" molecular device. From scheme **7** of Fig. 1 in paper¹³, we can see that BPBC system is readily accessible experimentally. The transmission spectrum for BPBC is plotted in Fig. 2. The transmission spectrum is dominated by the several peaks around the average Fermi energy. But these overlapping peaks are very broad comparing to those of BP transmission spectrum and they form a conductance plateau with high transmission probability within a broad range of the incident electron energy. These transmission peaks can be fitted by Lorenz lineshape with the broadening parameters σ varying from 0.3 to 0.8 eV, which are significantly larger than that of BP junction (typically 0.04 eV). There are two sharp transmission peaks at 1.81 and

2.29 eV above the average Fermi energy on the top of the plateau. These two sharp peaks are associated with MPSH orbital 48 and 49, and the four broad peaks correspond to the highest occupied MPSH orbital (HOMO, orbital 45), the lowest unoccupied MPSH orbital (LUMO, orbital 46), LUMO+1 (orbital 47) and orbital 50. HOMO and LUMO+1 come from the mixture of atomic orbitals from dithiocarbamate groups and BP molecule. HOMO is the bonding state, while LUMO+1 is the anti-bonding state.

According to the two rules of "robust" transmission spectrum, we can clearly see that the significant performance improvement is achieved for BPBC molecular wire junction comparing to BP junction system. This improvement is due to the stronger molecule-electrode coupling which results in the transmission peak broadening. The shift of peak position is the manifestation of the electronic structure of the dithiocarbamate group. In fact, in a model system with the apex Au atom of BP junction substituted by S atom, we also obtained significantly broadened transmission peaks, however the position of these peaks were exactly the same as those of BP junction. This result is consistent with the fact that S-Au bond is stronger than the N-Au bond, and the p orbital of S lays too deep below the electrode Fermi energy to manifest itself to the transmission spectrum. We also notice that the conjugation between the S_2C group and the end N atom of BP molecule plays a key role in the conductance improvement. As indicated in Fig. 3b, it is the π conjugation of the anchoring group which continues the conjugation from BP molecule directly to the metal.

Fig. 4 shows current-voltage (I-V) curve and conductance-voltage (dI/dV -V) characteristics of BP and BPBC molecular wire junctions. The conductance-voltage characteristics is computed via numerical differentiation of the I-V curve. The current dependence on the applied voltage is very different for BP and BPBC molecules reflecting the significant difference in the transmission spectra. The narrow resonance at the Fermi energy for BP molecular wire junctions leads to the steep increase of the electric current at the small applied voltage (≤ 0.5 V). The transmission for BP does not have any additional resonances in the energy range between -1 eV and 1 eV, therefore once the contribution of the first resonance has been included the current remains almost constant. The conductance-voltage characteristics reflects this behavior of the current-voltage curve. Conductance reaches its maximum at near zero bias voltage and then it sharply declines to very small values ($< 2.5 \mu S$). The overlap of the peaks in the transmission spectrum for BPBC molecular wire junction results in the

transmission coefficient, which is sufficiently large and does not change significantly with the variation of electron incident energies from -1 eV to 3 eV (relative to the average electrode Fermi energy). It leads to the structureless I-V and dI/dV -V characteristics for BPBC: current increases linearly with the voltage bias and the conductance remains constant within the broad range of bias voltage variations.

Although DFT plus NEGF represents the state-of-the-art transport theoretical model, the aim of the direct comparison of experimental and theoretical I-V characteristics remains illusive. The conductance enhancement factor (ration between BPBC and BP conductances) could be less sensitive to particular uncertainties of molecular-electrode interface geometry due the error cancelation. We thus suggest to use the conductance enhancement factor for comparing the results of theoretical calculations and of experimental measurements. Specifically, our calculations shows that the conductance enhancement factor at 1.0 V bias, where the conductance of both junctions are very stable (linear regime), is as large as 25. We notice that this conductance enhancement factor is consistent with the recent experiment,⁹ in which conductance of biphenyl with thiolate and dithiocarboxylate anchoring group was measured. The experimentally measured conductance of biphenyl dithiolate is about 40 times smaller than that of bipyridine.^{9,21} On the other hand, the conductance of the dithiocarboxylate linked molecular wire is enhanced by factor 1.4 with respect to the conductance of the thiolate anchored wire.⁹ If we assume that the conductance of BPBC and 4,4'-biphenyl bis(dithiocarboxylate) are the same within the order of magnitude, then our predicted enhancement factor qualitatively agrees with the existing experimental data.

C. Asymmetric anchoring

We use BPC molecular wire junction as a prototype system to study rectification of electron transport caused by the asymmetric anchoring groups, in which the left end of the bipyridine molecule is connected to the gold electrode via N-CS₂ linker whereas the right is attached to the electrode by N-Au bond. It is known experimentally that the force needed to break the N-Au bond is 0.8 nN, while the corresponding value for the S-Au bond is larger than 1.5 nN.²⁰ It indicates that the bonding between N and the gold surface is at least twice as weak as Au-S bond. With two S-Au chemical bonds on the left and with single N-Au bond on the right such hypothetical molecular wire junction would interact approximately

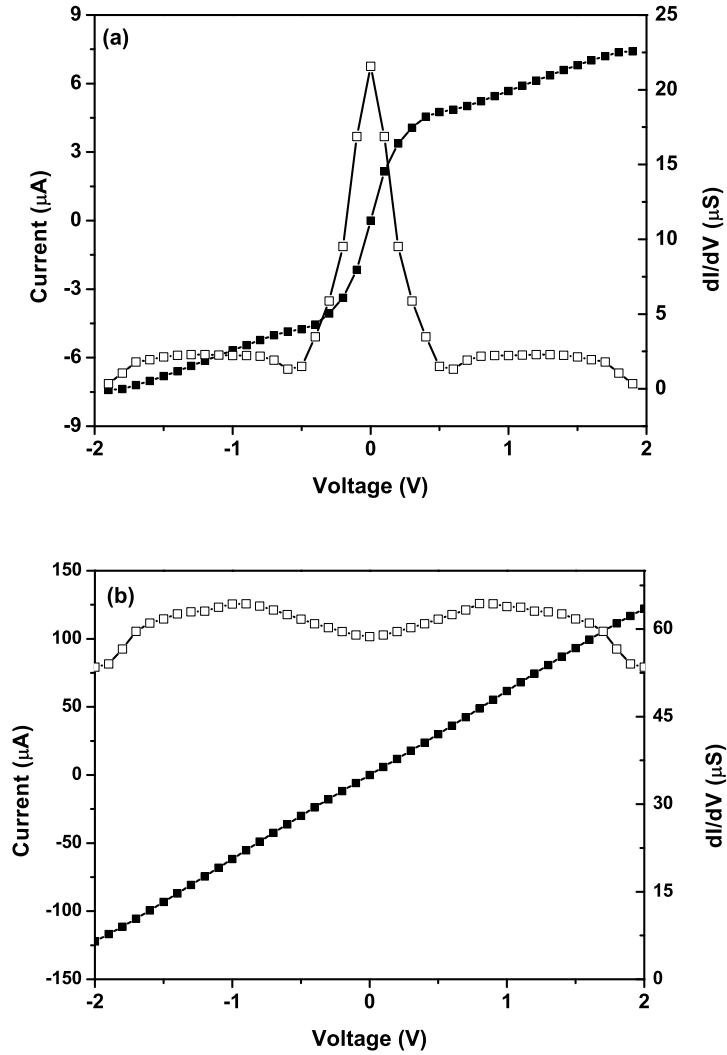


FIG. 4: Current-voltage (solid squares) and conductance-voltage (open squares) curves for (a) BP and (b) BPBC molecular wires

4 times stronger with the left electrode than with the right one.

The voltage dependent transmission spectrum is plotted in Fig. 5a. There are two main peaks located in the vicinity of the average electrode Fermi energy. These peaks are broad but their heights are much smaller than those of BPBC and BP molecules. The first peak crosses the average Fermi level energy and the second peak moves toward the Fermi energy as the voltage bias increases. The MPSH orbitals for BPC molecular wire junction are plotted

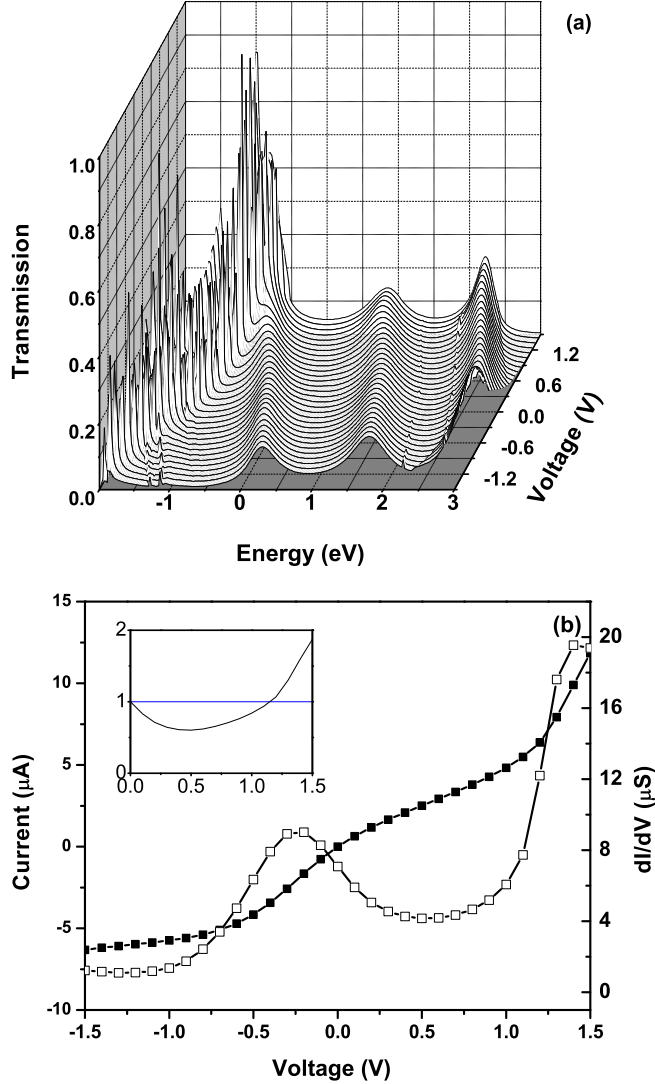


FIG. 5: (a) The transmission curves of BPC system at different bias voltages. (b) The current-voltage (solid squares) and conductance-voltage (open squares) curves of BPC system. Inset: rectification-voltage curve (abscissa – voltage; ordinate –rectification coefficient).

in Fig. 3c. Table I gives the corresponding eigenenergies. The electron transport through HOMO (orbital 43 in Fig. 3c) contributes to the first peak. The other two transmission peaks above the Fermi energy are associated with orbitals 44 and 47. Due to the strong coupling between molecule and left electrode, the transmission peaks are broad. On the other hand, because of the asymmetric electrode-wire coupling, the conjugation of the molecular orbitals

does not continue into the right electrode, which leads to the low transmission probability. In fact, the MPSH orbitals are asymmetric even if we focus on the region of BP molecule.

The current-voltage characteristic of BPC is plotted in Fig. 5b. As is expected from the transmission spectrum analysis, the I-V curve is asymmetric. Rectification coefficient $R(V) = |I(V)/I(-V)|$ is used to quantify the asymmetry of the molecular wire response on positive and negative applied voltage bias. $R = 1$ means that there is no rectification of the electric current. As shown in the inset of Fig. 5b, for BPC junction, $R < 1$ when the $V < 1.15$ V and $R > 1$ for the higher voltages. This means that the preferential direction for the current swaps with bias voltage: electrons flow easier from dithiocarbamate linked end toward nitrogen linked end at low applied voltage bias. When the voltage becomes larger than 1.15 V the preferential direction changes to the opposite.

The conductance of BPC molecular wire junction is small at large negative voltage bias, it grows up as the voltage increases. It reaches its first maximum (~ 9 S) at -0.3 V then decreases to its local minimum (~ 4 S) at 0.6 V. The conductance curve shows five fold increase within the voltage range of 0.5-1.5 V. This behavior of dI/dV -V can be explained from the variation of the transmission spectrum as a function of the bias voltage. We notice from Fig. 5a that the dependence of the transmission peaks upon the applied voltage bias follows the chemical potential of the electrode with stronger linkage (left electrode in our case). As was pointed out by Taylor *et al.*,¹⁹ this is the main reason for asymmetry in I-V characteristics for symmetric molecules. Electric current is obtained by the integration of the transmission spectrum from the left chemical potential μ_L to the right chemical potential μ_R (eq.(5)). When the bias voltage varies from 0.0 to -0.25 V, the transmission peak enter the integration range (from $\mu_L = -V/2$ to $\mu_R = V/2$). No new transmission peaks contribute to the integral for the negative voltage bias from -0.25 to -1.5 V. That is the reason why that maximum appears just below the zero bias voltage in the dI/dV -V curve. On the other hand, at the positive bias voltage side, at about 1.5 V, two transmission peaks enter the range of the integration and contribute to the integral, which generates the inversion of the rectification direction.

IV. CONCLUSIONS

Based upon the combination of DFT and NEGF, we have calculated the conductance for BP, BPBC and BPC molecular wire junctions. Our calculations show that dithiocarbamate linking to the Au electrode leads to the strong molecule-electrode coupling, which is able to continue the π conjugation from the molecule to the metal. The overlap of the peaks in the transmission spectrum for BPBC junction results in the transmission coefficient, which is sufficiently large and does not change significantly with the variation of electron incident energies from -1 eV to 3 eV (relative to the average electrode Fermi energy). The electric current increases linearly with the voltage bias and the conductance remains constant within the broad range of bias voltage variations for BPBC molecular wire junction. Our calculations thus demonstrate that the conductance of BP molecular wire can be significantly improved by using dithiocarbamate anchoring group. A conductance enhancement by factor of 25 in the linear regime is predicted, which is qualitatively consistent with the experimental data. We propose to use dithiocarbamate anchoring group to make asymmetric molecular wire junction. We studied the rectification of the electron transport caused by the asymmetric anchoring groups on the example of BPC wire. We show that BPC molecular wire junction rectifies the electric current by factor close to 2. The preferential direction for the current flow undergoes the inversion at critical voltage 1.15 V.

ACKNOWLEDGMENTS

The authors are grateful to M. Gelin, L. Sita, A. Vedernikov and J. Yang for helpful discussions. Part of the calculations were performed on computational facilities at the Laboratory of Bond Selective Chemistry, USTC. This work was partially supported by the Mitsubishi Chemical Corporation.

¹ Nitzan, A.; Ratner, M. A. *Science* **2003**, 300, 1384.

² Joachim, C.; Ratner, M. A. *Proc. Natl. Acad. Sci. U.S.A.* **2005**, 102, 8801.

³ Xue, Y.; Ratner, M. A. *Phys. Rev. B* **2003**, 68, 115406.

⁴ Ke, S.-H.; Baranger, H. U.; Yang, W. *J. Am. Chem. Soc.* **2004**, 126, 15897.

- ⁵ Basch, H.; Cohen, R.; Ratner, M. A. *Nano Lett.* **2005**, 5, 1668-1675.
- ⁶ Ke, S.-H.; Baranger, H. U.; Yang, W. *J. Chem. Phys.* **2005**, 123, 114701.
- ⁷ Tulevski, G. S.; Myers, M. B.; Hybertsen, M. S.; Steigerwald, M. L., Nuckolls, C. *Science* **2005**, 309, 591.
- ⁸ Sijaj, M.; McBreen, P. H. *Science* **2005**, 309, 588.
- ⁹ Tivanski, A. V.; He, Y.; Borguet, E.; Liu, H.; Walker, G. C.; Waldeck, D. H. *J. Phys. Chem. B* **2005**, 109, 5398.
- ¹⁰ Guo, X.; Small, J. P.; Klare, J. E.; Wang, Y.; Purewal, M. S.; Tam, I. W.; Hong, B. H.; Caldwell, R.; Huang, L.; O'Brien, S.; Yan, J.; Breslow, R.; Wind, S. J.; Hone, J.; Kim, P.; Nuckolls, C. *Science* **2006**, 311, 356.
- ¹¹ Venkataraman, L.; Klare, J. E.; Tam, I. W.; Nuckolls, C.; Hybertsen, M. S.; Steigerwald, M. L. *Nano Lett.* **2006**, ASAP Article.
- ¹² He, J.; Chen, B.; Flatt, A. K.; Stephenson, J.J.; Doyle, C.D.; Tour, J.M. *Nature Materials* **2006**, 5, 63.
- ¹³ Zhao, Y.; Perez-Segarra, W.; Shi, Q.; Wei, A. *J. Am. Chem. Soc.* **2005**, 127, 7328.
- ¹⁴ Metzger, R. M. *Chem. Rev.* **2003**, 103, 3803.
- ¹⁵ Aviram, A.; Ratner, M. A. *Chem. Phys. Lett.* **1974**, 29, 277.
- ¹⁶ Morales, G.; Jiang, P.; Yuan, S.; Lee, Y.; Sanchez, A.; You, W.; Yu, L. *J. Am. Chem. Soc.* **2005**, 127, 10456.
- ¹⁷ Elbing, M.; Ochs, R.; Koentopp, M.; Fischer, M.; von Hanisch, G.; Weigend, F.; Evers, F.; Weber, H. B.; Mayor, M. *Proc. Nat. Acad. Sci.* **2005**, 102, 8815.
- ¹⁸ Derosa, P. A.; Guda, S.; Seminario J. M. *J. Am. Chem. Soc.* **2003**, 125, 14240.
- ¹⁹ Taylor, J.; Brandbyge, M.; Stokbro, K. *Phys. Rev. Lett.* **2002**, 89, 138301.
- ²⁰ Xu, B.; Xiao, X.; Tao, N. J. *J. Am. Chem. Soc.* **2003**, 125, 16164.
- ²¹ Xu, B.; Tao, N. J. *Science* **2003**, 301, 1221.
- ²² Tada, T.; Kondo, M.; Yoshizawa, K. *J. Chem. Phys.* **2004**, 121, 8050.
- ²³ Perez-Jimenez, A. J. *J. Phys. Chem. B* **2005**, 109, 10052.
- ²⁴ Wu, X.; Li, Q.; Huang, J.; Yang, J. *J. Chem. Phys.* **2005**, 123, 184712.
- ²⁵ Brandbyge, M.; Mozos, J.-L.; Ordejon, P.; Taylor, J.; Stokbro, K. *Phys. Rev. B* **2002**, 65, 165401.
- ²⁶ Soler, J. M.; Artacho, E., Gale, J.; Garcia, A., Junquera, J.; Ordejon, P.; Sanchez-Portal, D. *J.*

Phys.: Condens. Matter **2002**, 14, 2745.

²⁷ Troullier, N; Martins, J. L. *Phys. Rev. B* **2001**, 43, 1993.

²⁸ Perdew, J. P.; Zunger, A. *Phys. Rev. B* **1981**, 23, 5048.

²⁹ Ramachandran, G. K.; Hopson, T. J.; Rawlett, A. M.; Nagahara, L. A.; Primak, A.; Lindsay, S. M. *Science* **2003**, 300, 1413.

³⁰ Hu, Y.; Zhu, Y.; Gao, H. *Phys. Rev. Lett.* **2005**, 95, 156803.

³¹ Donhauser, Z.; Mantooth, B.; Kelly, K.; Bumm, L.; Monnell, J.; Stapleton, J.; Price, D.; Rawlett, A.; Allara, D.; Tour, J. *Science* **2001**, 292, 2303.